Chapter 55
Improving Pulse Oximetry Accuracy by Removing Motion Artifacts from Photoplethysmograms Using Relative Sensor Motion: A Preliminary Study

R.W.C.G.R. Wijshoff, M. Mischi, P.H. Woerlee, and R.M. Aarts

Abstract To expand applicability of pulse oximetry in low-acuity ambulatory settings, the impact of motion on extracted parameters as saturation (SpO_2) and pulse rate (PR) needs to be reduced. We hypothesized that sensor motion relative to the skin can be used as an artifact reference in a correlation canceller to reduce motion artifacts in photoplethysmograms (PPGs), in order to improve SpO_2 and PR measurements. This has been proven true in in vivo measurements, where forehead PPGs have been obtained while subjects are walking on a treadmill and relative sensor motion has been measured via self-mixing interferometry. By using relative motion in a normalized least mean square algorithm, the standard deviation of SpO_2 and PR errors is on average reduced by 31 % and 13 %, respectively.

55.1 Introduction

Pulse oximetry is widely applied in medical care to measure peripheral arterial oxygen saturation (SpO_2) and pulse rate (PR). SpO_2 is derived from red (RD) and infrared (IR) photoplethysmograms (PPGs), and PR from either.

At present, use of pulse oximeters is spreading in low-acuity ambulatory settings, e.g., to obtain temporal SpO_2 patterns of chronic lung disease (CLD) patients during activities of daily living. Temporal SpO_2 patterns can be used to advance

R.W.C.G.R. Wijshoff (✉) • M. Mischi • R.M. Aarts
Department of Electrical Engineering, Signal Processing Systems group, Eindhoven University of Technology, Den Dolech 2, Eindhoven 5612 AZ, The Netherlands
e-mail: R.W.C.G.R.Wijshoff@tue.nl; M.Mischi@tue.nl; R.M.Aarts@tue.nl

P.H. Woerlee
Patient Care Solutions, Philips Research, High Tech Campus 34, Eindhoven 5656 AE, The Netherlands
e-mail: Pierre.Woerlee@philips.com

S. Van Huffel et al. (eds.), *Oxygen Transport to Tissue XXXV*, Advances in Experimental Medicine and Biology 789, DOI 10.1007/978-1-4614-7411-1_55,

understanding of CLD and to improve oxygen therapy [1–3]. In addition, heart rate variability (HRV) can be derived from a PPG, e.g., to assess dynamic characteristics of the patient's autonomic nervous system [4].

As PPGs are highly susceptible to motion, ambulatory oximetry and PPG derived HRV can be severely affected by motion artifacts [1, 4]. We hypothesized that motion artifacts in PPGs correlate with sensor motion relative to the skin. Therefore, relative sensor motion can be used as a reference for motion artifacts in a correlation canceller, in order to reduce motion artifacts in PPGs. This enables more reliable beat-to-beat SpO_2 and PR measurements. Relative sensor motion is measured via self-mixing interferometry (SMI) in a laser diode, which has been added to a commercially available forehead pulse oximetry sensor.

This chapter focuses on reflective pulse oximetry sensors, because these sensors are most practical to measure relative sensor motion. Commercially available forehead sensors have been employed to obtain PPGs during walking from healthy volunteers. Forehead measurements have the advantage of being less affected by vasoconstriction, which can cause weakly pulsatile PPGs to be measured peripherally, e.g., in the fingers [5]. Additionally, forehead sensors are more stable during motion as compared to finger sensors [6].

55.2 Methods

Forehead PPGs were measured in five healthy male volunteers (35.6 ± 11.3 years) while walking on a treadmill at speeds between 4 and 8 km/h to generate repetitive motion artifacts that can be expected in ambulatory settings. Each speed was maintained for 2 min and was preceded and followed by a 1-min period during which the subject stood still. Figure 55.1 gives an overview of the measured signals. Forehead

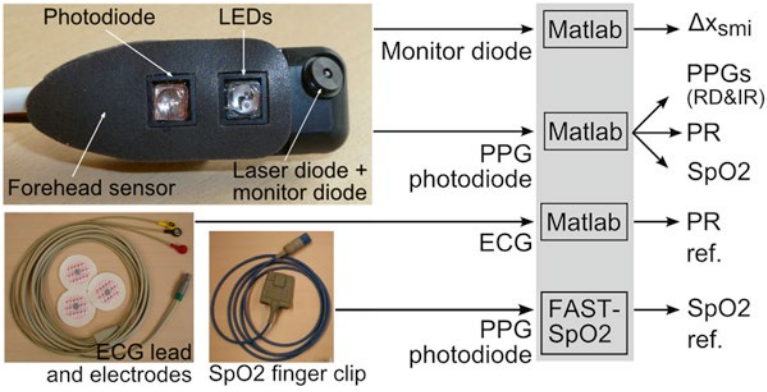

Fig. 55.1 Overview of the measured signals: forehead PPGs (RD and IR) are obtained with a commercial sensor to which a laser diode has been added to measure relative sensor motion; PR and SpO_2 are derived from the forehead PPGs; HR is determined from a single-lead ECG as PR reference; an SpO_2 reference is obtained from the index finger using the FAST-SpO_2 algorithm

PPGs were obtained with a Nellcor Oxisensor II RS-10, which was attached using an adhesive and a headband. SpO_2 and PR were derived on a beat-to-beat basis: SpO_2 via the ratio of the DC-normalized RD and IR pulse amplitudes [7] and PR from the IR PPG by defining a pulse at the average of the time instances of the systolic slope and the diastolic and systolic portions. References for SpO_2 and PR were obtained via an SpO_2 clip on the index finger and a single-lead ECG, respectively. Motion of the reference SpO_2 clip was minimized during walking. The Philips FAST-SpO_2 algorithm was used to obtain the reference SpO_2. Heart rate (HR) was derived from the R-peaks in the ECG.

To measure motion of the forehead sensor with respect to the skin via SMI, an 850 nm vertical-cavity surface-emitting laser diode (VCSEL) with a monitor diode was added to the commercial forehead sensor (Fig. 55.1). The algorithm to measure motion via SMI is explained in detail in [8] and will only be described shortly. During relative motion, the laser light that is backscattered by the skin is Doppler shifted with Doppler phase φ_d. Furthermore, the laser injection current is amplitude modulated. Therefore, when the Doppler-shifted light re-enters the laser cavity, the monitor diode measures a signal proportional to $\sin(\varphi_d)$ around the modulation frequency and a signal proportional to $\cos(\varphi_d)$ around the second harmonic of the modulation frequency. After demodulating these signals to baseband and normalizing their amplitudes, the sensor motion Δx_{smi} can be determined from the Doppler phase by counting the number of Doppler cycles:

$$\Delta x_{smi}[k] = \frac{1}{2\pi}\,\mathrm{unwrap}\left(\arctan 2\left(\frac{\sin(\varphi_d[k])}{\cos(\varphi_d[k])}\right)\right) \approx \sum_{l=0}^{k} f_d[l]\Delta\tau, \tag{55.1}$$

with discrete time index k, Doppler frequency $f_d[k]$ (Hz), and sampling time $\Delta\tau$ (s). Further, arctan2(.) refers to an arctangent implementation that takes into account in which quadrant the Doppler signals are located. Each phase change of 2π rad in $\varphi_d[k]$ corresponds to a full Doppler cycle, and the sign of the phase change depends on the direction of motion. Motion cannot be measured in absolute units, because the time-varying angle between laser beam and skin is not exactly known.

Relative motion is subsequently used in a normalized least mean square (NLMS) algorithm [9] to reduce the motion artifacts in the PPGs (Fig. 55.2). Here, all signals are down-sampled to 100 Hz. First, the PPG photodiode signal $v_{PD}[k]$ is passed through a 0.3-Hz high-pass filter (HPF) and delayed. Second, the motion artifact estimate is subtracted, giving $e_o[k]$. The artifact estimate is obtained from $\Delta x_{smi\text{-}s}[k] = 10^{-5}\Delta x_{smi}[k]$ (of comparable magnitude as $v_{PD}[k]$) via FIR filter $\mathbf{h}[k]$ of $N_f = 101$ coefficients. The low frequent signal is added to $e_o[k]$ again to determine SpO_2 from the cleaned PPGs. The optimum FIR filter is obtained iteratively via:

$$\mathbf{h}[k+1] = \mathbf{h}[k] + \frac{\mu}{a + \left\|\Delta\mathbf{x}_{smi-s}[k]\right\|^2} e_o[k]\Delta\mathbf{x}_{smi-s}[k], \tag{55.2}$$

with step-rate parameter $\mu = 5.10^{-3}$ and $a = 10^{-6}$. The filtered PPG has been delayed by $(N_f - 1)/2$ samples to allow for symmetrical FIR filters.

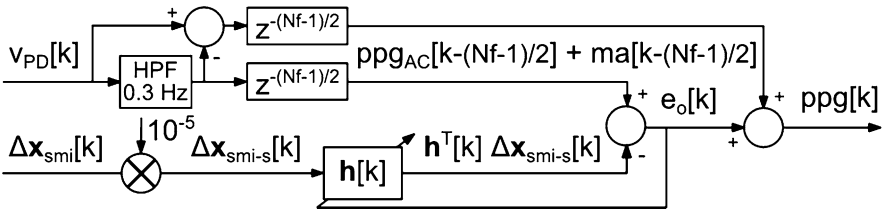

Fig. 55.2 NLMS structure: motion artifacts ma[k] are reduced in the photodiode signal $v_{PD}[k]$ by subtracting the artifacts which are estimated from relative sensor motion $\Delta x_{smi}[k]$ filtered by an FIR filter of N_f coefficients

55.3 Results

As shown in the red PPG's spectrogram in Fig. 55.3e, walking causes additive motion components at the full swing (±1 Hz) and step frequencies (±2 Hz), as well as their harmonics. These motion components result in an amplitude modulation of the PPG as shown by the dashed curve in Fig. 55.3a. Consequently, PR and SpO_2 oscillate around the references, as shown by their differences ΔPR (circles, Fig. 55.3b) and ΔSpO_2 (circles, Fig. 55.3c), SpO_2 showing the strongest oscillation. Furthermore, relative sensor motion (Fig. 55.3d) indicates that the sensor moves at the step rate.

By using relative sensor motion as an artifact reference in an NLMS algorithm (Fig. 55.2), motion artifacts can be largely removed from the PPGs, as shown by the spectrogram of the cleaned red PPG in Fig. 55.3f. Here, a strong reduction of the step-rate component at ±2 Hz has been achieved, and a small reduction of the motion components at ±1 Hz and ±3 Hz. As a result, the cleaned PPG's amplitude is more stable (solid curve in Fig. 55.3a), and the oscillatory pattern in PR and SpO_2 determined from the cleaned PPGs is reduced (stars in Fig. 55.3b and c, respectively). The magnitude frequency response of the converged FIR filter that achieves this artifact reduction shows resonances at ±1 Hz, ±2 Hz, and ±3 Hz (Fig. 55.3g).

The effect of motion on PR and SpO_2 and the performance of the NLMS algorithm vary over the subjects (Fig. 55.4). The difference with the reference (mean ± SD) for PR (ΔPR) and SpO_2 (ΔSpO_2) is determined in baseline when the subject is standing still before and after walking (triangles), during walking (circles), and after the NLMS algorithm has been applied (stars). Only measurement results are shown (12 out of 25) in which PR did not coincide with step rate and in which the RMS amplitude of Δx_{smi} during motion was at least three times larger compared to baseline. Motion increases the PR SD most in subjects 1 and 5 and by 264 % on average; it does not introduce a bias. Motion increases the SpO_2 SD in all subjects and by 42 % on average, except for subject 3 in which the SpO_2 SD decreases during motion. In subject 5 also the baseline SpO_2 bias varies over the measurements. Removal of motion artifacts reduces the SpO_2 SD in all cases and by 31 % on average, but the PR SD only in seven out of 12 cases and by 13 % on average.

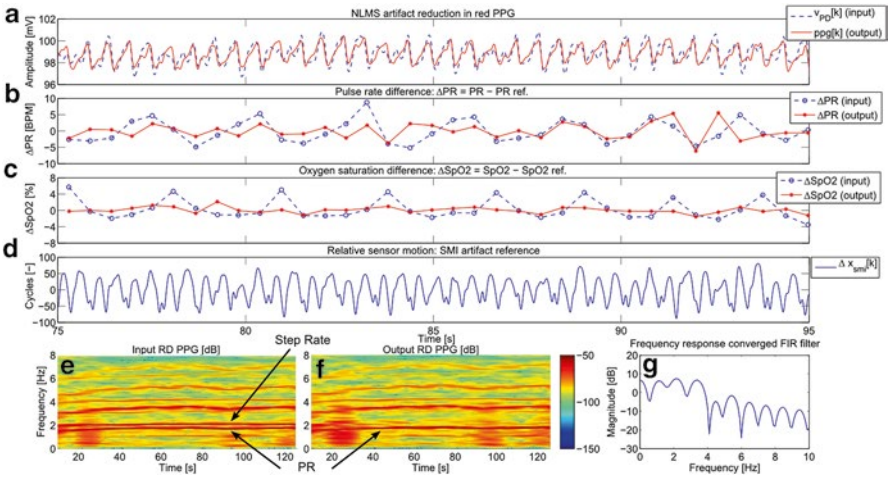

Fig. 55.3 PPG motion artifacts in subject 5 caused by walking at 6 km/h (**a**, *dashed curve*) can be reduced strongly (**a**, *solid curve*) via NLMS by using relative sensor motion (**d**) as an artifact reference; comparing the difference between PR and PR ref. (ΔPR) (**b**) and SpO_2 and SpO_2 ref. (ΔSpO_2) (**c**) resulting from the corrupted (*circles*) and cleaned (*stars*) PPGs shows a larger improvement for SpO_2 than for PR; spectrograms of the corrupted (**e**) and cleaned (**f**) RD PPG show a reduction of motion components at ±1 Hz, ±2 Hz, and ±3 Hz, and the magnitude frequency response of the converged FIR filter shows resonances at these frequencies (**g**)

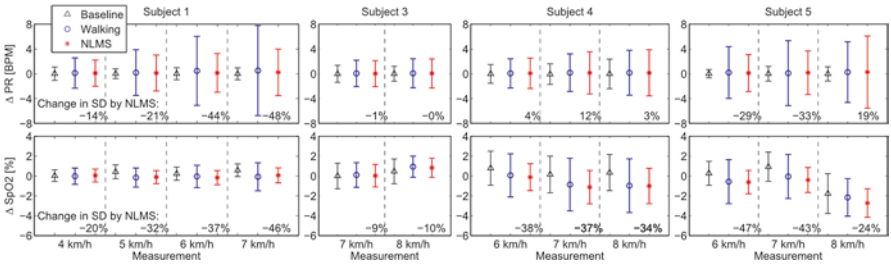

Fig. 55.4 Difference (mean ± SD) between PR and PR ref. (ΔPR), and SpO_2 and SpO_2 ref. (ΔSpO_2), in baseline when the subject is standing still (*triangles*), during walking (*circles*), and after NLMS artifact reduction (*stars*); change in SD as a result of NLMS artifact reduction is shown as a percentage

55.4 Discussion

The NLMS algorithm has only been applied to measurements in which PR and step rate did not coincide and in which the relative motion signal was sufficiently strong. When PR and step rate coincide, the algorithm removes both motion artifact and PPG. This drawback is inherent to correlation cancelation. A relative motion signal

of poor quality may result from a small sensor to forehead motion. Differences in relative motion may result from intersubject differences in walking and variations in sensor contact force. As the same type of headband is used for all subjects, the head's circumference determines the force exerted on the sensor.

Figure 55.3 shows that the steady motion component in the PPG can be strongly reduced via the NLMS algorithm. However, this implementation of the NLMS algorithm is unable to correct for fast and relatively large sensor displacements, as happens at 20 s in Fig. 55.3e and f. Furthermore, in some subjects, PR is observed via SMI, in which case the NLMS algorithm can affect the PR component in the PPG.

The forehead and finger SpO_2 time traces are not identical in shape, even during baseline, which complicates their synchronization. Therefore, ΔSpO_2 is partly caused by synchronization issues, e.g., causing ΔSpO_2 in subject 3 to be smaller during motion compared to baseline. Even so, Fig. 55.4 shows that walking has a moderate effect on PR and SpO_2 derived from forehead PPGs, which can be a result of step rate being close to PR and the stable measurement site [6]. Further, Fig. 55.4 shows that the improvement in PR is smaller compared to the improvement in SpO_2. This indicates that the algorithm can improve the amplitude of the PPG waveform, but cannot perfectly recover its shape. Finally, intersubject differences in the effect of walking on PPGs, PR, and SpO_2 can be a result of differences in sensor positioning and fixation, skin dynamics, anatomy, and the way of walking.

55.5 Conclusions

If PR and the motion frequency do not coincide, relative sensor motion measured via SMI can be used as an artifact reference in an NLMS algorithm to reduce motion artifacts in a PPG, which can improve SpO_2 and PR measurements. Furthermore, the forehead is a stable position to measure PPGs during walking, as walking has a moderate effect on forehead PPGs and derived SpO_2 and PR.

Acknowledgments This work was supported by NL Agency, IOP Photonic Devices, IPD083359 HIP – Hemodynamics by Interferometric Photonics.

References

1. Barratt CW, Vyas H, Hayes-Gill BR, Crowe JA, Flatman D (2007) Detection of previously unrecognized daytime desaturation in children with chronic lung disease. J Med Eng Technol 31(2):101–108
2. Cutaia M (2002) Ambulatory monitoring of oxygen saturation in chronic lung disease: optimizing long-term oxygen therapy. Clin Pulm Med 9(6):297–305
3. Zhu Z, Barnette RK, Fussell KM, Michael Rodriguez R, Canonico A, Light RW (2005) Continuous oxygen monitoring–a better way to prescribe long-term oxygen therapy. Respir Med 99(11):1386–1392

4. Lu S, Zhao H, Ju K et al (2008) Can photoplethysmography variability serve as an alternative approach to obtain heart rate variability information? J Clin Monit Comput 22(1):23–29
5. Branson RD, Mannheimer PD (2004) Forehead oximetry in critically ill patients: the case for a new monitoring site. Respir Care Clin N Am 10(3):359–367
6. Yamaya Y, Bogaard HJ, Wagner PD, Niizeki K, Hopkins SR (2002) Validity of pulse oximetry during maximal exercise in normoxia, hypoxia and hyperoxia. J Appl Physiol 92(1):162–168
7. Palreddy S (1997) Signal processing algorithms. In: Webster JG (ed) Design of pulse oximeters. Taylor & Francis Group, New York
8. Wijshoff RWCGR, Mischi M, Veen J, Van der Lee AM, Aarts RM (2012) Reducing motion artifacts in photoplethysmograms by using relative sensor motion: phantom study. J Biomed Opt 17(11):117007–1–15
9. Haykin S (1996) Least-mean-square algorithm. In: Adaptive filter theory, 3rd edn. Prentice-Hall, Upper Saddle River